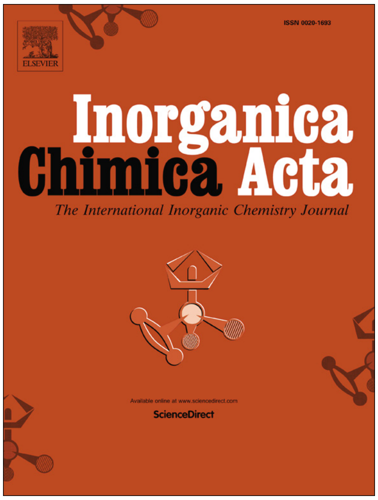

Research paper

Mononuclear Nickel (II) and Copper (II) Coordination Complexes Supported by Bispicen Ligand Derivatives: Experimental and Computational Studies

Nirupama Singh, Jens Niklas, Oleg Poluektov, Katherine M. Van Heuvelen, Anusree Mukherjee

PII: S0020-1693(16)30505-9
DOI: http://dx.doi.org/10.1016/j.ica.2016.09.001
Reference: ICA 17246

To appear in: *Inorganica Chimica Acta*

Received Date: 21 July 2016
Revised Date: 2 September 2016
Accepted Date: 3 September 2016

Please cite this article as: N. Singh, J. Niklas, O. Poluektov, K.M. Van Heuvelen, A. Mukherjee, Mononuclear Nickel (II) and Copper (II) Coordination Complexes Supported by Bispicen Ligand Derivatives: Experimental and Computational Studies, *Inorganica Chimica Acta* (2016), doi: http://dx.doi.org/10.1016/j.ica.2016.09.001

Mononuclear Nickel (II) and Copper (II) Coordination Complexes Supported by Bispicen Ligand Derivatives: Experimental and Computational Studies

Nirupama Singh[1]*, Jens Niklas*[2]*, Oleg Poluektov*[2]*, Katherine M. Van Heuvelen*[3]***, Anusree Mukherjee*[1]***

1. Department of Chemistry, University of Alabama in Huntsville, 301 Sparkman Drive, Huntsville, AL 35899
2. Chemical Science and Engineering Division, Argonne National Laboratory, 9700 S. Cass Avenue, Lemont, IL 60439
3. Department of Chemistry, Harvey Mudd College, 301 Platt Blvd. Claremont, CA, 91711

ABSTRACT

The synthesis, characterization and density functional theory calculations of mononuclear Ni and Cu complexes supported by the N,N'-Dimethyl-N,N'-bis-(pyridine-2-ylmethyl)-1,2-diaminoethane ligand and its derivatives are reported. The complexes were characterized by X-ray crystallography as well as by UV−visible absorption spectroscopy and EPR spectroscopy.

The solid state structure of these coordination complexes revealed that the geometry of the complex depended on the identity of the metal center. Solution phase characterization data are in accord with the solid phase structure, indicating minimal structural changes in solution. Optical spectroscopy revealed that all of the complexes exhibit color owing to d-d transition bands in the visible region. Magnetic parameters obtained from EPR spectroscopy with other structural data suggest that the Ni(II) complexes are in pseudo-octahedral geometry and Cu(II) complexes are in a distorted square pyramidal geometry. In order to understand in detail how ligand sterics and electronics affect complex topology detailed computational studies were performed. The series of complexes reported in this article will add significant value in the field of coordination chemistry as Ni(II) and Cu(II) complexes supported by tetradentate pyridyl based ligands are rather scarce.

Introduction

Low molecular weight coordination complexes of late transition metals bound by nitrogen rich ligands are very important because of their pivotal roles in bioinorganic chemistry and potential catalytic applications.[1-4] Transition metal complexes supported by tetradentate polypyridyl ligands are well-studied because of their role in bioinorganic chemistry.[5-9] In coordination chemistry, polydentate ligands from the bispicen family with amine and pyridine functionalities (N2/Py2) have also received significant attention for their role in hydrocarbon oxidation with high selectivity.[10-12] These N2/Py2 ligands are particularly interesting as they support different topologies[13] namely, *cis-α*, *cis-β* and *trans*.[14-19] These ligands are also attractive candidates for designing homogeneous catalysts as ease of synthesis allows systematic investigation of structural-functional relationship of the catalysts. Efforts in our research group focus on designing ligand architecture by introducing different electronic and steric properties on the N,N’-Dimethyl-N,N’-bis-(pyridine-2-ylmethyl)-1,2-diaminoethane ligand (L^1, commonly known as BPMEN) and studying the effect of ligand topology in complex geometry (Chart 1). The ligand has been widely studied for nonheme iron dioxygenase models, but the effects of ligand topology on the electronic properties of late transition metals such as Ni and Cu metal complexes remain largely unexplored.[6,20,21] Herein, we describe the synthesis, characterization and electronic properties of mononuclear Ni(II) and Cu(II) complexes supported by N2/Py2 ligands: [Ni(L^1)Cl$_2$] (**1**), [Ni(L^{1}Q)Cl$_2$] (**2**) and [Ni(L^2)Cl$_2$] (**3**), [Cu(L^1)ClO$_4$]ClO$_4$ (**4**), [Cu(L^{1}Q)ClO$_4$]ClO$_4$ (**5**) and [Cu(L^2)ClO$_4$]ClO$_4$] (**6**) (L^1 = N,N'-Dimethyl-N,N'-bis-(pyridine-2-ylmethyl)-1,2-diaminoethane), L^{1}Q = N,N'-Dimethyl-N,N'-bis-(quinoline-2-ylmethyl)-1,2-diaminoethane, L^2 = N,N'-Dimethyl-N,N'-bis-(3,4-dimethoxypyridine-2-ylmethyl)-1,2-diaminoethane). Ligand L^1 is known to support Ni(II) and Cu(II) complexes with chloride counter anions.[21,22] This paper reports first synthesis and structural characterization of a new Ni complex supported by the L^{1}Q ligand. In addition, we also synthesized a series of Cu(II) complexes with perchlorate counter anions. Moreover, this paper also reports the synthesis of a new variation of the N2/Py2 ligand L^2, which has electron-donating substituent in the pyridyl moiety and the respective Ni and Cu complexes.

Chart 1 N2/Py2 ligands of bispicen family studied

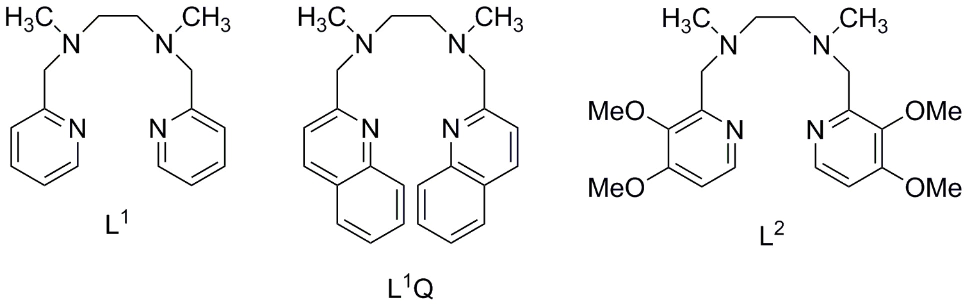

Results and Discussion

Synthesis of ligand and metal complexes

The synthesis of L^1 ligand has been reported previously and other ligands were synthesized by slightly modifying the reported procedure.[23] Initially, one equivalent of picolyl chloride hydrochloride was treated with two equivalents of strong base to generate the picolyl chloride. The freshly synthesized picolyl chloride was immediately mixed with one equivalent of N,N'-dimethylethylenediamine in the presence of sodium hydroxide to synthesize ligand L^1. The variations on the ligand architecture were achieved by using substituted picolyl chloride derivatives (Scheme 1). The new ligand moiety L^2 was prepared by using 2-(chloromethyl)-3,4-dimethoxypyridine hydrochloride as a starting material. For ligand L^1Q, 2-(chloromethyl)-pyridine hydrochloride was substituted by 2-(chloromethyl)-quinoline hydrochloride. The ligands were characterized by ^{1}H-NMR spectroscopy and purity of ligands was suitable for metal complex synthesis.

Scheme 1 Synthesis of ligands (quinoline ring is shown in dashed format)

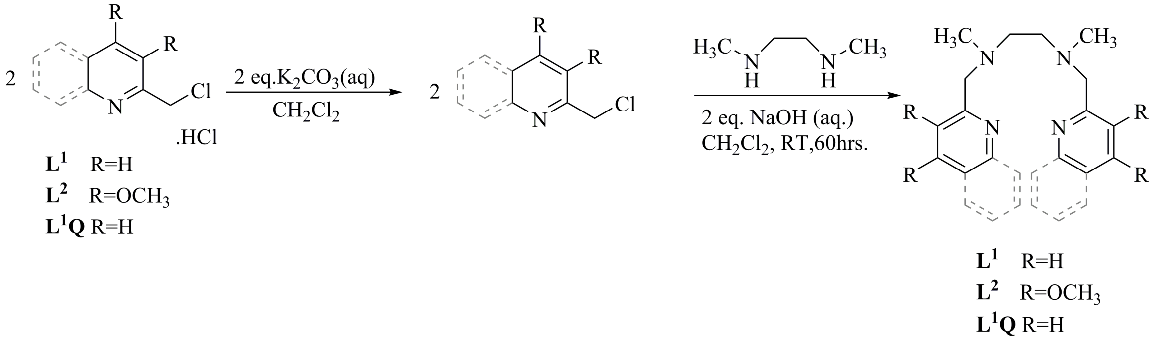

The metal complexes were synthesized by mixing the ligand and the corresponding metal salt in methanol (Scheme 2) with the exception of complex **1**, which was synthesized following a published procedure.[21] In order to synthesize the Ni-compounds **1** - **3**, $NiCl_2$•$6H_2O$ was used as a starting material. In case of Cu-compounds **4** - **6**, $Cu(ClO_4)_2$•$6H_2O$ allowed us to isolate the products in higher yields. All of these compounds were analyzed by spectroscopic methods and attempts were made to obtain single crystals suitable for X-ray diffractions. We were able to obtain the first crystal structure of compound **2**. We were also able to crystalize compound **4** from a different crystallization condition than known in literature[20] (*vide infra*). Crystallographic parameters of these two compounds are summarized in Table 1.

Scheme 2 Synthesized Cu- and Ni-complexes of N2/Py2 ligand system

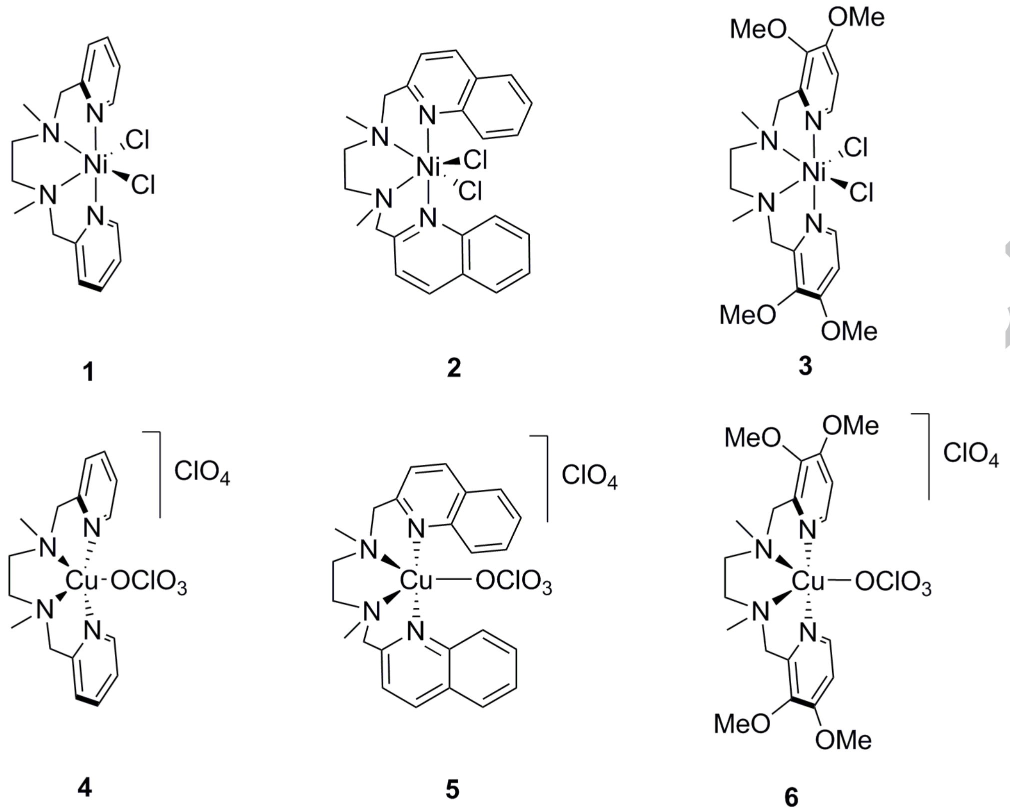

Table 1: Crystallographic parameters and details of structure determination for complex **2** and **4**

Compound	**2**	**4**
Formula	$C_{24}H_{26}Cl_2N_4Ni$	$C_{16}H_{22}Cl_2CuN_4O_8$
$D_{calc.}$/ g cm^{-3}	1.493	1.554
μ/mm^{-1}	1.132	1.358
Formula Weight	500.10	482.29
Colour	green	blue
Shape	prism	prism
Max Size/mm	0.48	0.52
Mid Size/mm	0.39	0.27
Min Size/mm	0.23	0.15
T/K	100(2)	100(2)
Crystal System	orthorhombic	triclinic
Space Group	Pbcn	P-1
a/Å	15.410(3)	8.8875(11)
b/Å	8.1028(16)	12.6671(15)
c/Å	17.820(4)	18.538(2)
$\alpha/^{\circ}$	90	85.075(2)
$\beta/^{\circ}$	90	84.259(2)
$\gamma/^{\circ}$	90	84.619(2)
V/Å^3	2225.1(8)	2061.2(4)
Z	4	4
Z'	0.5	2
$\Theta_{min}/^{\circ}$	2.286	1.620
$\Theta_{max}/^{\circ}$	29.695	30.622
Measured Refl.	17050	44284
Independent Refl.	3140	12390
Reflections Used	2698	10235
R_{int}	0.0343	0.0322
Parameters	184	681
Restraints	45	171
Largest Peak	0.571	1.320
Deepest Hole	-0.417	-1.098
GooF	1.051	1.034
wR_2 (all data)	0.0971	0.1144
wR_2	0.0905	0.1055
R_1 (all data)	0.0451	0.0565
R_1	0.0371	0.0441

Structural Characterization

X-ray Crystallography

Single crystals suitable for X-ray diffraction studies were obtained for the complex **2** from methanol. Complex **2** showed nickel in a pseudo-octahedral geometry with four coordination sites occupied by the nitrogen atoms of the ligand and two other coordination sites were occupied by chloride ions (Figure 1). The planes of the two quinoline rings are positioned at an angle of 169.50º relative to each other. The corresponding angles between quinoline rings and Ni–Cl bonds are 85.90º. The angle between both chloride counter ions and Ni metal ion was observed as 92.99º. It was also noted that the Ni-N (quinoline) bond distances (2.2857 Å) are longer than Ni-N (amine) bond distance (2.1284 Å). The Ni-N bond lengths of compound **2** are in accord with other reported complexes and suggest the central Ni(II) ion is in the high spin configuration in octahedral geometry.[21,24-26] In complex **2**, the ligand L^{1}Q moiety supports a *cis*-topology, and substituting the pyridine ring with the quinoline does not lead to any drastic changes in the ligand topology. But, the Ni-N bond length corresponding to pyridine/quinoline ring was elongated in complex **2** that can be attributed to steric requirements of quinoline ring structure. However, the Ni-N (amine) bond distance was shorter in complex **2** than in complex **1**.

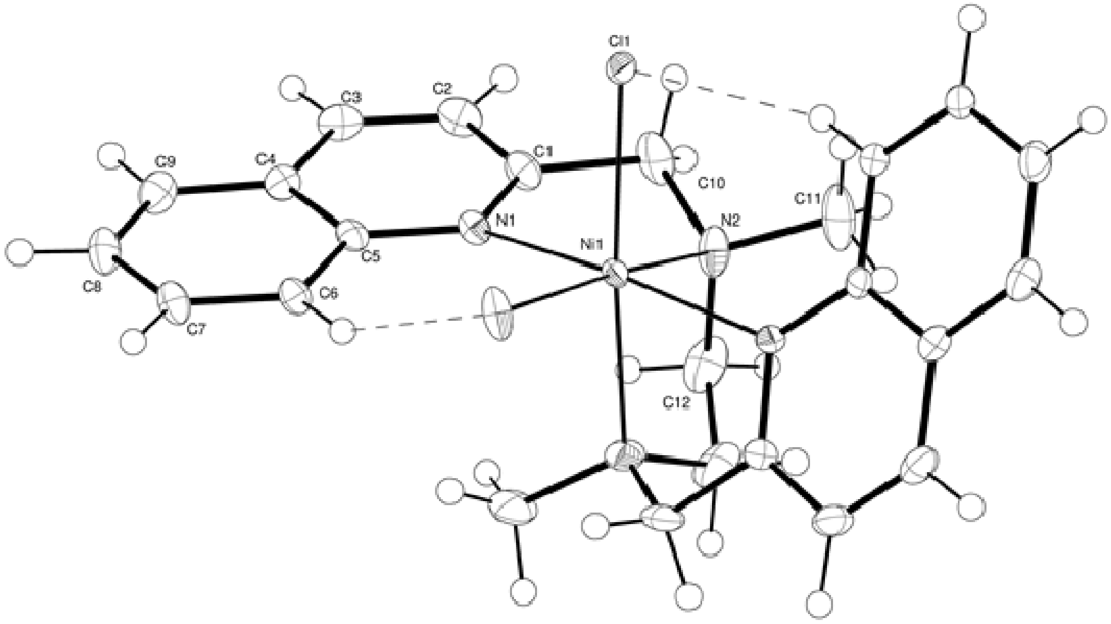

Figure 1. ORTEP view of complex **2** [Ni(L^{1}Q)(Cl)$_2$]. Hydrogen bonding observed between Cl atom and H6 atom of the pyridine ring is shown by dotted line.

Table 2 Selected bond distances (Å) and bond angles (in Degrees) for **2** and **4** from crystal structures

	C22[Ni(L^1Q)Cl_2] (2)		
Atom	**Distance/ Å**	**[Ni(L^1)Cl_2] (1)[21]**	**Bond Angle/ degrees**
Ni1-Cl1	2.3774(5)	2.4332(13)	92.99(Cl1-Ni1-Cl1)
Ni1-N1	2.2857(15)	2.094(3)	85.90(N1-Ni1-Cl1)
Ni1-N2	2.1284(15)	2.160(4)	95.50(N2-Ni1-N1)
	[Cu(L^1)(ClO_4)$_2$] (4)		
Atom	**Distance/ Å**	**[Cu(BPMEN)ClO_4][20]**	**Bond Angle/ degrees**
Cu1-O1	2.2459(17)	2.246(4)	91.64(N1-Cu1-O1)
Cu1-N1	1.9901(17)	1.996(3)	82.63(N1-Cu1-N2)
Cu1-N2	2.0260(18)	2.031(3)	146.45(N2-Cu1-N4)
Cu1-N3	2.0251(17)	2.028(3)	86.86(N3-Cu1-N2)
Cu1-N4	1.9976(17)	2.000(3)	167.82(N1-Cu1-N3)

Single crystals of complex **4** suitable for X-ray diffraction were grown from a solution in MeCN and hexane vapor. In compound **4**, the central metal Cu is in a distorted square-pyramidal geometry (= 0.35; where = 0.00 for a perfect square pyramidal and = 1.00 for a trigonal bipyramidal geometry)[27,28] with four coordination sites occupied by nitrogen atoms of the ligand and the fifth axial site occupied by one oxygen atom from the perchlorate counter ion (Figure 2). In complex **4**, the second perchlorate ion is in the outer-sphere. This result agrees with a previous study of [Cu(BPMEN)(ClO_4)]ClO_4, but it is strikingly different than the geometry observed in the Ni-analogue (**1**).[20] This distinct change in geometry of the metal complex may be attributed to the central metal Cu(II) ion that may prefer a square pyramidal geometry over distorted octahedral geometry to minimize Jahn-Teller distortion. A comparison of selected bond lengths and angles is shown in Table 2.

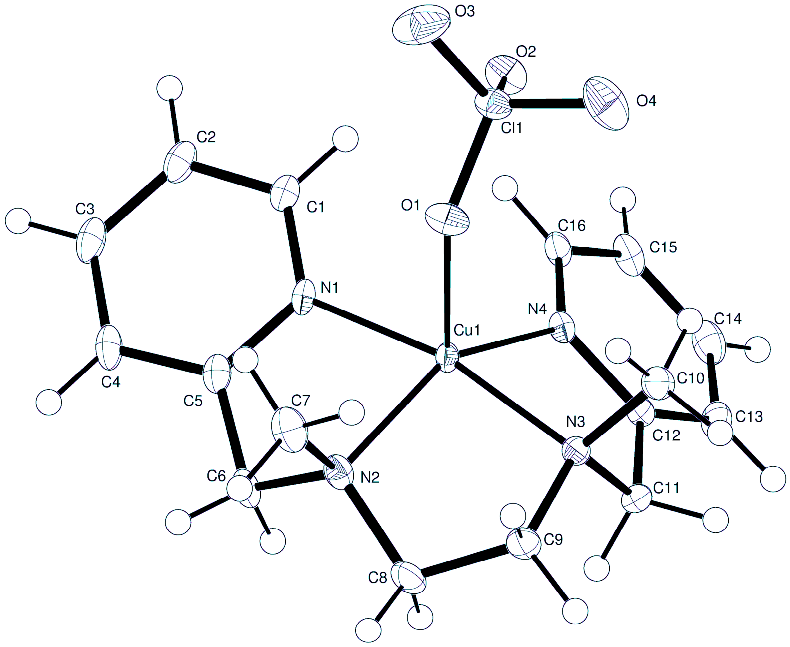

Figure 2. ORTEP view of complex **4** [Cu(L^1)(ClO$_4$)]ClO$_4$]

Computational Investigations of 1- 6

Structures of **1 – 6** were optimized using density functional theory as implemented in the Gaussian 09 software package using the M06 functional[29] and the 6-311G(D) basis set[30] on the metal. The 6-31G(d) basis set was used on all other atoms.[31] The crystal structure of **2** was used as a starting point for geometry optimization of all Ni-complexes **1 - 3**. Calculations considered Ni(II) in both the high spin and low spin configurations, and in all cases the high spin case best reproduced experimental data. Hence, only the high spin results are considered herein. The crystal structure obtained for **4** was used as the initial geometry for the Cu-complexes **4 - 6**.

The calculated bond distances in complex **1** match reasonably well with the previously reported crystal structure.[21] The optimized structures of **1** and **2** reproduce the experimentally observed elongation of the Ni-N(pyridine/quinoline) bonds in **2** compared to **1** (Table 3). Octahedral compounds coordinated by this family of tetradentate ligands can adopt one of three ligand topologies: *cis*-α, *cis*-β, and *trans* (Scheme 3A).[13] We evaluated the relative stabilities of these isomers of **1** using DFT. The *cis*-α configuration of **1** is considerably more stable than both the *cis*-β (10.4 kcal/mol) and *trans* (8.0 kcal/mol) isomers. Based on these observations we conducted theoretical studies of all three *cis*- , *cis*-β and *trans* isomers of **2** and **3**. For complex **2**, the *cis*-α isomer was more stable than the *cis*-β and *trans* isomers by 2.1 and 1.6 kcal/mol, respectively. The same holds true for complex **3**, in which the *cis*-α is more stable than both the *cis*-β (3.8 kcal/mol) and *trans* (6.1 kcal/mol) isomers. To summarize, DFT calculations suggest that the *cis*- configuration is the most stable form of the complexes **1**, **2** and **3**.

Scheme 3 Possible conformers of the metal complexes arising due to ligand topology

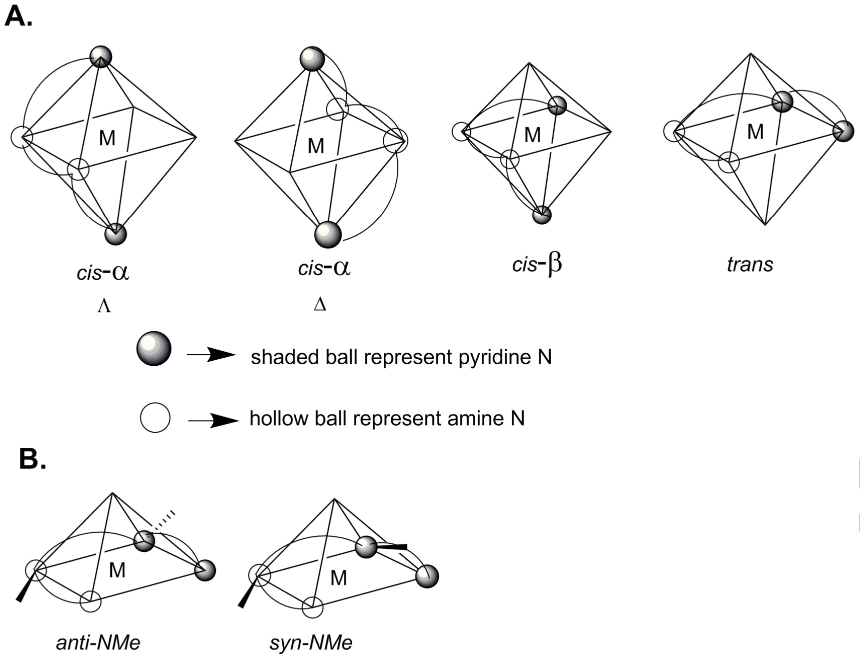

We also used density functional theory to explore the possible optical isomers of the Ni-complexes (Figure 3). Experimental data show that complex **1**, crystallizes as the Λ enantiomer,[32] whereas **2** crystallizes as the Δ enantiomer (this work). As **3** has not yet been crystallized, we performed theoretical studies considering the and enantiomers of complex **3** and found that the two enantiomers have essentially identical energies, differing by only 0.1 kcal/mol.

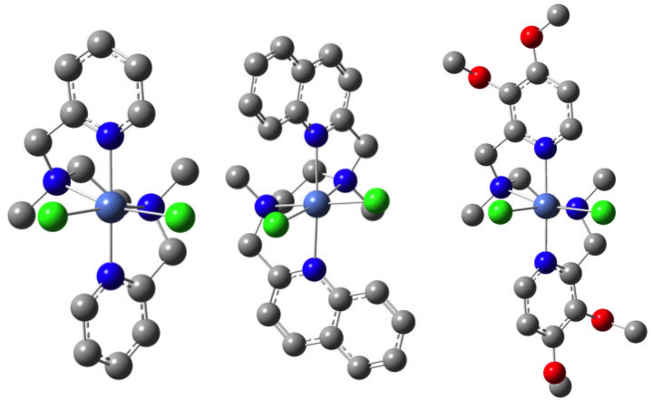

Figure 3. Optimized geometries of **1**, **2** and **3**. Hydrogen atoms are omitted for clarity.

Table 3. Experimental and Calculated Structural Parameters for **1 - 3**. All bond lengths reported in angstroms (Å).

	1 (L^1)	**1** (L^1)	**2** (L^1Q)	**2** (L^1Q)	**3** (L^2)
	Exp[21]	Calc	Exp	Calc	Calc
Ni1-Cl1	2.4332(13)	2.367	2.3774(5)	2.340	2.384
Ni1-Cl2	2.4332(13)	2.367	2.3774(5)	2.340	2.377
Ni1-N1(pyr)	2.094(3)	2.095	2.2857(15)	2.310	2.088
Ni1-N2	2.160(4)	2.213	2.1284(15)	2.168	2.199
Ni1-N3	2.160	2.213		2.168	2.200
Ni1-N4(pyr)	2.094	2.095		2.310	2.090

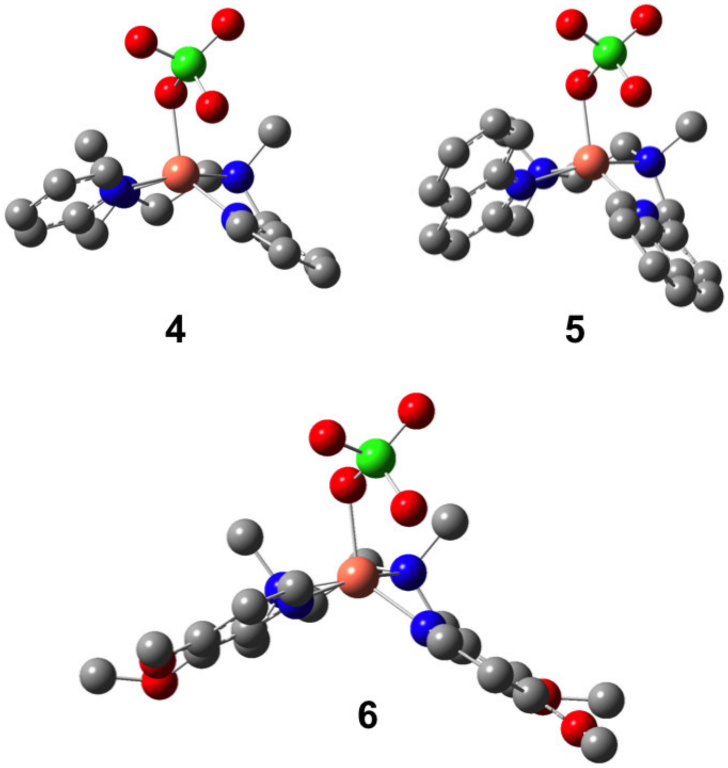
4

5

6

Figure 4. Optimized geometries of *syn* isomers of **4 – 6**. Hydrogen atoms are omitted for clarity.

The similarities between **4**, **5**, and **6** regarding the optical and EPR spectral properties *(vide infra)* suggest the three complexes share a similar coordination environment. Therefore, the crystal structure of **4** was used as a starting point for geometry optimizations of all three Cu-complexes (Figure 4) and calculated structural parameters are shown in Table 4. Calculated bond distances are in reasonable agreement with experimental data. We attribute minor discrepancies between experimental and calculated bond lengths to crystal packing forces.[33] The Cu-complexes adopt a distorted square pyramidal geometry in which the tetradentate ligand occupies the basal plane. As noted by González and coworkers,[20] the substituents in the ligand architecture supporting the complex can adopt different geometries. The two methyl groups on the backbone of L^1 can assume a *syn* or *anti* configuration (Scheme 3B). In the *syn* isomer, the two N-CH_3 groups are on the same side of the plane, and this isomer is observed in the crystal structure of **4** (Figure 2, C7 and C10). These N-CH_3 groups are on opposite sides of the ligand in the *anti*-isomer. González and coworkers reported DFT studies of **4** showing the *syn* and *anti*- isomers were very close in energy and thus were likely to exist in equilibrium when in solution. In agreement with this result, our studies of *syn* and *anti*- isomers of **4** – **6** show minimal energy differences (< 1 kcal/mol) between the two isomers. A comparison of the two isomers shows the *anti*-isomer is associated with a slight contraction of the Cu-O(perchlorate) and Cu-N(pyridine/quinoline) bonds with a concomitant elongation of the Cu-N(amine) bonds. This elongation in the *anti*- versus the *syn*- isomer is most dramatic in the cases of L^1Q and L^2 and may be attributed to the steric constraint imposed by the ligand.

Table 4. Experimental and Calculated Structural Parameters for **4 - 6.** All bond lengths reported in angstroms (Å).

	4 (L^1)	**4** (*syn*- L^1)	**4** (*anti*- L^1)	**5** (*syn* L^1Q)	**5** (*anti* L^1Q)	**6** (*syn*-L^2)	**6** (*anti*- L^2)

	Exp (this work)	Calc	Calc	Calc	Calc	Calc	Calc
Cu1-O	2.2459	2.290	2.010	2.049	1.978	2.256	2.035
Cu1-N1(pyr)	1.9901	1.980	1.981	2.028	2.004	1.979	1.986
Cu1-N2	2.0260	2.112	2.270	2.053	2.153	2.116	2.263
Cu1-N3	2.0251	2.021	2.135	2.052	2.278	2.023	2.100
Cu1-N4(pyr)	1.9976	2.069	1.971	2.272	1.972	2.028	1.971

Optical Spectroscopy

In methanol, complexes **1**, **2** and **3** all gave colored solution with an optical band in the visible region with weak intensity (Figure 5). The optical spectrum of complex **1** was identical with previously reported spectral data,[34] and all absorption data including the peak position and molar absorptivity are summarized in the Table 5. The band in the near-UV region is characteristic of an intra-ligand charge transfer transition[35] and the bands in the visible region 600 – 900 nm with weak intensity were assigned to d-d transitions at the metal center. The transition at 600-900 nm region could be assigned to $^3A_{2g} \rightarrow {}^3T_{1g}$ electronic transition from a Ni-complex in octahedral geometry.[36,37] The optical spectra of complex **1**, **2** and **3** matches reasonably well with other reported complexes of high spin Ni(II) in an octahedral geometry.[38-40] In complex **2**, the peak in the visible region is slightly red-shifted from 601 nm of complex **1** to 630 nm in complex **2**. This observation can be rationalized using the knowledge obtained from the crystal structure. The steric bulk of the quinoline results in elongated metal-ligand distances that decreases the ligand field strength of ligand L^1Q and lowers the energy of d-d transitions. The absorption spectrum for complex **3** is similar to complex **1**. The peaks in the visible region are comparable to those observed for complex **1**, suggesting that ligand field strength in complex **1** and complex **3** are very similar.

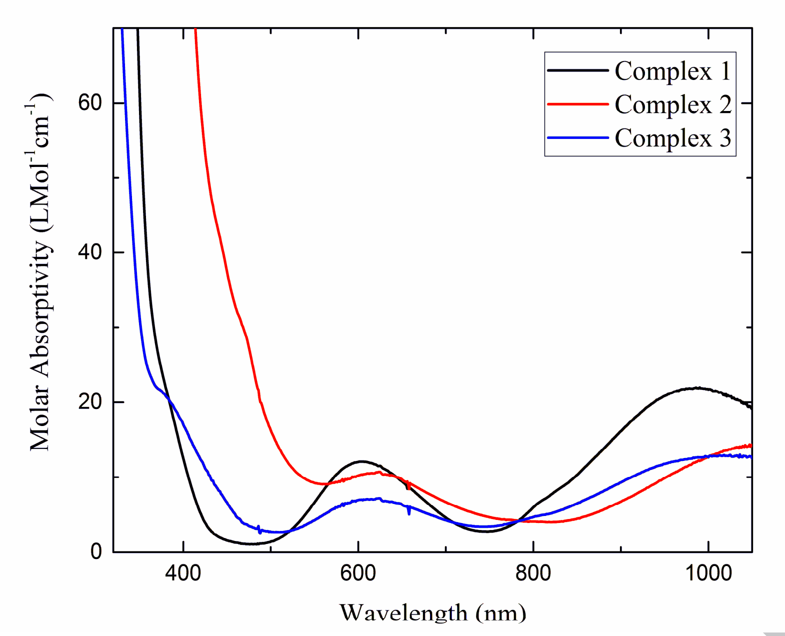

Figure 5. UV-Visible spectra of complex **1** (black), **2** (red) and **3** (blue) in methanol at 25 °C (Concentration used: 8 mM)

The electronic absorption spectra for complex **4**, **5** and **6** were recorded in methanol and in acetonitrile (Figure 6). In acetonitrile, complexes **4** and **6** exhibit a deep blue color due to a strong absorption peak at 624 nm and 626 nm respectively. For complex **5** the absorption peak appears at 628 nm along with a broad shoulder at 900 nm corresponding to a bluish-green color. In methanol, complex **4** shows an absorption maximum at 624 nm, exactly as observed in acetonitrile. Complex **5** the transition band appeared at 651 nm and a shoulder peak at 440 and 470 nm. The absorption maximum with complex **6** in methanol appears at 634 nm. The absorption features in all three complexes are characteristics of mononuclear Cu(II) compounds supported by nitrogen enriched ligands in square pyramidal geometry.[41-44] The red-shifts observed in methanol are minor (*ca.* 10 - 20 nm) and may be attributed to the slight distortion of the geometry but as observed in EPR spectra (*vide infra*), all of the complexes remain in distorted square pyramidal geometry.[42] It is known in the literature that mononuclear Cu(II) complexes in a trigonal-bipyramidal geometry usually exhibit absorption maxima at longer wavelength *ca*. 700 - 980 nm.[45-48]

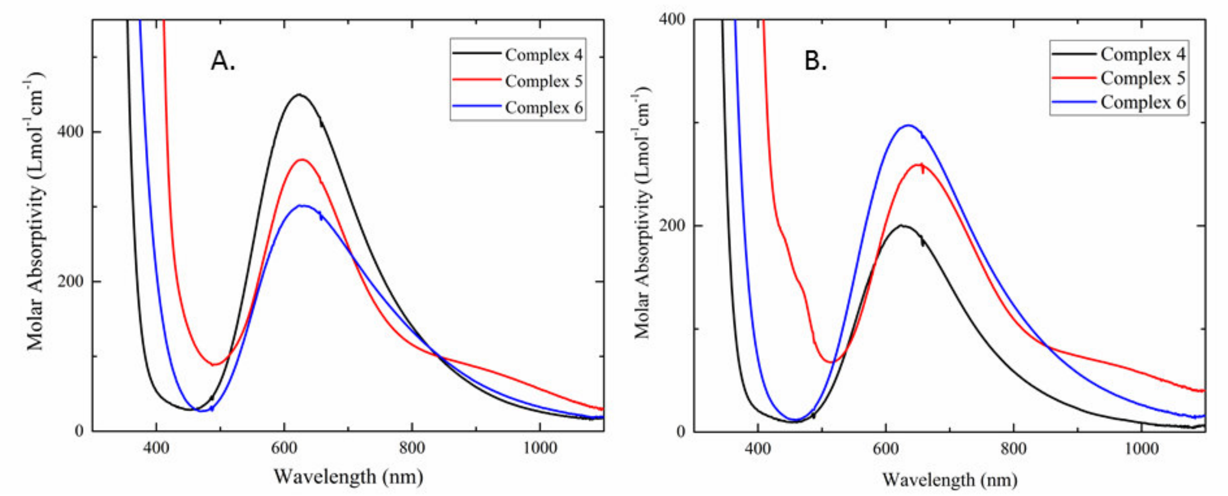

Figure 6. UV-Visible spectra of complex **4**(black), **5**(red) and **6**(blue) in acetonitrile (panel A) and methanol (panel B) at 25 °C.

Electron Paramagnetic Resonance Spectroscopy

EPR spectroscopy was employed to characterize the compounds in solution. The magnetic resonance parameters obtained by simulation of the continuous wave (CW) X-band EPR measurements on compounds **1** - **6** are summarized in Table 5. Frozen solutions of the Ni-complexes **1**, **2** and **3** in methanol remained EPR silent, which is expected assuming that they have a high spin nickel ion in Ni(II) oxidation state (d^8 configuration, S = 1). This is in agreement with the data obtained from crystal structure, theoretical calculations and optical absorption spectroscopy that supports a high spin Ni(II) ion in pseudo-octahedral geometry. The high spin configuration of the Ni-complexes was also supported by magnetic susceptibility measurements using the Gouy method. At room temperature, the effective magnetic moment for complex **1**, **2** and **3** were measured to be 2.92, 2.95 and 3.28 B.M., respectively. These values are in excellent agreement with other reported octahedral Ni(II) complexes in similar coordination environments.[49,50]

EPR measurements on frozen solutions of Cu-complexes **4**, **5** and **6** in dichloromethane/acetonitrile (3:1) solvent system all gave distinct signals, characteristic of mononuclear Cu(II) complexes in d^9 configuration with S = ½ (Figure 7). EPR spectra recorded in methanol as solvent gave similar results, but were less resolved. These results suggest that solvent interaction is weak and that the overall geometry is very similar in both solvents. The frozen solution EPR spectra of all Cu(II)-complexes showed a $g_{.}$ value (~ 2.21) significantly higher than the $g_{.}$ value (~ 2.05) and resolved ^{63,65}Cu hyperfine structure for $A_{\parallel}$ (~ 176 x 10^{-4} cm^{-1} > $A_{.}$ (Cu has two isotopes with nuclear spin I=3/2, which have very similar magnetic moments and are not resolved in our spectra). EPR parameters obtained for our complexes match reasonably well with other reported mononuclear Cu(II) complexes in square-pyramidal geometry.[42,51] These type of EPR spectra commonly termed as 'usual' axial signal[52] indicate that these three complexes have mononuclear Cu(II) center in a square pyramidal geometry or elongated octahedral geometry with $d_{x^2-y^2}$ ground state.[28,53-56] The EPR data in frozen solution suggest that the crystal structure obtained for complex **4** is retained in solution. The magnetic resonance parameters for **5** and **6** are very close to those of complex **4.** This is not surprising, since the only structural difference between complexes **4** and **6** is the presence of the two methoxy groups attached to each of the pyridyl moieties. For complex **5**, the similarity of the magnetic parameters reflects that introducing the quinoline moiety instead of the pyridyl moiety does not lead to significant changes in electronic structure of Cu and its coordinating environment. However, a small increase in linewidth from complex **4** to the complexes **5** and **6** is observed, which may be attributed to a wider distribution of small variations in local site geometry (strain) in frozen solution due to the steric effects of the substituents. Super-hyperfine structure due to the four ^{14}N nuclei coordinating the central Cu(II) ion are not resolved in our EPR spectra for any of these three complexes. In combination with the crystal structure of **4**, it can be assumed that all three Cu-complexes are in square-pyramidal geometry, but an elongated octahedral geometry arising due to solvent coordination in the frozen solution cannot be totally excluded with certainty at this point.

Table 5: Electronic parameters of compounds **1** - **6**

	Absorption Maxima nm, ($M^{-1}cm^{-1}$)	Solvent	g values[a]		Cu Hyperfine coupling constants (10^{-4} cm^{-1})[a]	
			g.	g.,	A.	A.
1	400 (sh), 601(15), 800(sh), 981(28)	MeOH	Silent			
2	392 (sh), 636 (10), 1026 (11	MeOH	Silent			
3	390 (sh), 611 (10), 803(sh) 969 (17)	MeOH	Silent			
4	624 (200)	MeOH	2.213	2.053	175	31
	624 (450)	MeCN				
5	440 (sh), 465 (sh), 651(258)	MeOH	2.229	2.055	176	18
	626 (362)	MeCN				
6	634 (295)	MeOH	2.219	2.053	177	25
	625 (301)	MeCN				

a. All EPR measurements were performed in DCM:MeCN solvent mixture (3:1). Cu hyperfine coupling constants are given in 10^{-4} cm^{-1} for the ^{63}Cu isotope. The perpendicular value A. has a larger error than the parallel value, since the hyperfine structure is not clearly resolved. Lifting the assumption of axial g-tensor and Cu A-tensor slightly improved the fit of simulation to experiment. However, for a reliable determination of the rhombicity EPR spectra at different frequencies would be required, thus the simulations were performed assuming axial g-tensor and Cu hyperfine tensors. In addition, it was assumed for the simulation that the principal g-tensor axes are collinear with the Cu A-tensor principal axes.

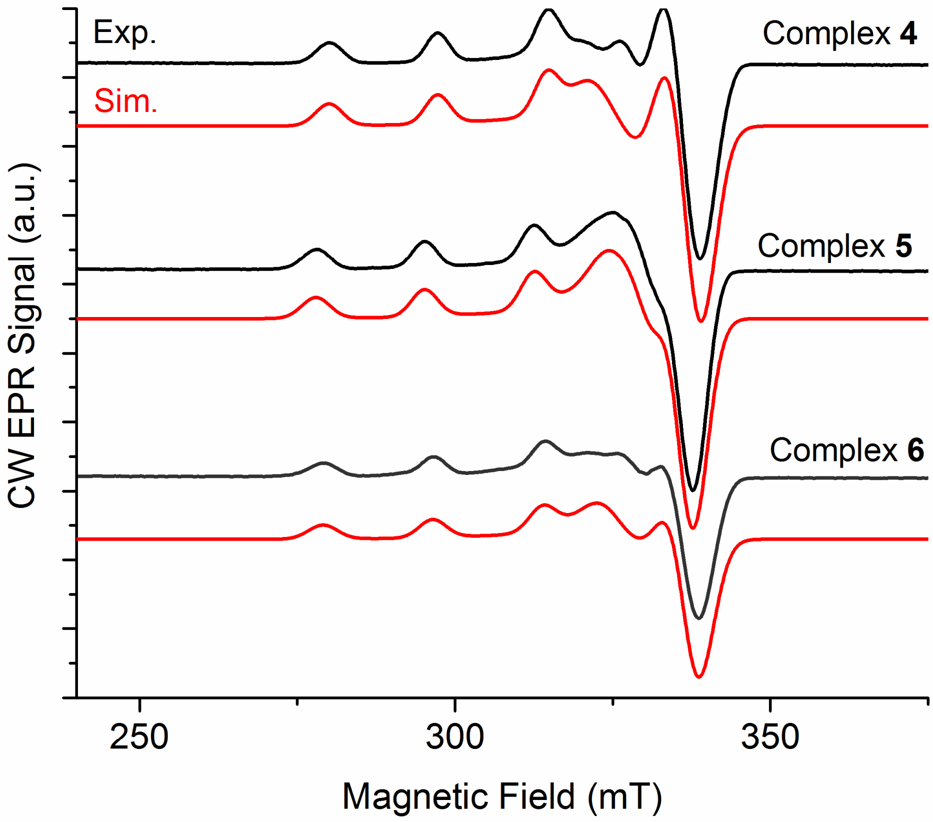

Figure7. CW X-band EPR spectra obtained from complex **4**, **5** and **6** in dichloromethane-acetonitrile solvent mixture (3:1). Spectra shown in black are the experimental spectra. Spectra in red are the corresponding simulation. Simulation parameters are summarized in Table 5.

Conclusion

The synthesis of late transition metal coordination compounds is of significant value and has been extensively researched. However, many previously reported Cu(II) and Ni(II) complexes are supported by tetradentate ligands derived from Schiff bases.[25,57,58] There is a paucity of Ni and Cu complexes supported by the N2/Py2 ligand family. In this study we offer the first report of a series of Ni and Cu complexes supported by the same N2/Py2 ligand family. Electronic properties of all these complexes were investigated in solution, and theoretical calculations were performed to investigate the stabilities of different ligand topologies in the metal complexes. This study reports the first synthesis and crystal structure of a Ni-complex (**2**) in a sterically demanding tetradentate ligand environment. Other than a very few crystal structures[59-61], no detailed investigations of Ni(II) and Cu(II) complexes supported by the N2/Py2 ligand family and their solution phase characterization have been reported prior to this work. Current efforts in the group are focused investigating the reactivity of these complexes in hydrocarbon oxidation using earth abundant oxidants and correlating structure and function. Overall these mononuclear Cu and Ni complexes have the potential to serve as functional models for metalloenzymes and to serve as homogeneous catalysts.

Experimental Section

Materials. All reagents and solvents were purchased from Sigma-Aldrich and Fisher chemicals and directly used in synthesis without further purification unless otherwise mentioned. The solvents for NMR measurement were purchased from Cambridge Isotopes Laboratory and used as received. Metal complex syntheses and spectroscopic measurements were performed using commercially available anhydrous solvents. ***Caution***: *Although no problems were encountered in this work, transition metal perchlorates are potentially explosive. They should be prepared in small quantities and handled with care.*

Physical Methods. All ^{1}H-NMR experiments were performed in the listed deuterated solvents on a Varian Inova 500MHz instrument at 25 ºC. Electronic absorption spectra were measured using a Cary 8454 UV-Vis Spectrophotometer, Agilent technologies. All UV-Vis samples were prepared in a quartz cells with an optical pathlength of 1 cm. The mass spectrometry (ESI-MS) was performed with Thermo scientific LTQ Orbitrap XL Hybrid FT Mass Spectrometer in a positive ionization mode. IR data were collected using a ThermoScientific Nicolet i55 FT-IR spectrometer equipped with an iD5 ATR accessory. Elemental Analysis was performed by Atlantic Microlab, Inc., (Norcross, Georgia, United States). Continuous wave (CW) X-band (9 - 10 GHz) EPR experiments were carried out with a Bruker ELEXSYS II E500 EPR spectrometer (Bruker Biospin, Rheinstetten, Germany), equipped with a TE$_{102}$ rectangular EPR resonator (Bruker ER 4102st). A helium gas-flow cryostat (ICE Oxford, UK) and. an intelligent temperature controller (ITC503) from Oxford Instruments, UK, were used for measurements at cryogenic temperatures (T = 50 K). Data processing was done using Xepr (Bruker BioSpin, Rheinstetten) and Matlab 7.11.1 (The MathWorks, Inc., Natick) environment. Simulations were performed using the EasySpin software package (version 5.0.20).[62] The room temperature magnetic susceptibilities in the solid state were measured using Johnson Matthey magnetic susceptibility balance (model MK I#7967). The appropriate diamagnetic corrections of the molar magnetic susceptibilities were applied using Pascal's constant.[63]

Crystallographic Details. For complex **2**, green prism-shaped crystal were recrystallised from methanol by slow evaporation. A single crystal (0.48×0.39×0.23 mm) was selected and mounted on a loop with paratone oil on a Bruker APEX-II CCD diffractometer. The crystal was kept at $T = 100(2)$ K during data collection. The structure was solved with the **XT** structure solution program,[64] using direct and dual-space solution methods and by using **Olex2**,[65] as the graphical interface. The model was refined with version of **ShelXL-97**[66] using Least Squares minimisation. For complex **4**, blue prism-shaped crystals were recrystallised from a mixture of hexane and acetonitrile by vapor diffusion. A suitable crystal (0.52×0.27×0.15 mm) was selected and mounted on a loop with paratone oil on a Bruker APEX-II CCD diffractometer. The crystal was cooled to $T = 100(2)$ K during the data collection. The structure was solved with **ShelXT** using direct and dual-space solution methods and by using **Olex2** as the graphical interface.[64,65] The model was refined with version 2013-4 of **ShelXL-97**[66] using Least Squares minimization.

Computational Details

DFT geometry optimization and frequency calculations were performed using Gaussian 09 Revision D.01[67] as implemented on the Extreme Scientific and Engineering Discovery Environment (XSEDE).[68] Optimized structures were obtained using unrestricted hybrid functional M06.[29] The 6-311G(d) basis set[30] was used for the metal and the 6-31G(d) basis set[31] was used for all other atoms. Complex **2** converged to C2 symmetry and all other complexes converged to the C1 point group. Energy minimized coordinates are provided in the supporting information.

Synthesis of Ligands

L^1 [N,N'-Dimethyl-N,N'-bis-(pyridine-2-ylmethyl)-1,2-diaminoethane]. The ligand L^1 was synthesized via previously reported procedure.[23] A solution of potassium carbonate (2.55 g, 18.45 mmol) in 10 mL water was dropwise added to the aqueous solution of 2-(chloromethyl)-pyridine hydrochloride (1.5 g, 9.15 mmol in 10 mL). After about 30 min. of stirring at room temperature, the reaction mixture was extracted with dichloromethane (3 × 20 mL). The combined organic extracts were dried over anhydrous sodium sulfate. The solution was filtered and the solvent was removed under vacuum. The resulted residue was then dissolved in dichloromethane (10 mL). The dichloromethane solution of 2-chloromethyl-pyridine was added dropwise to a solution of N,N'-Dimethylethylenediamine (0.471 mL, 5.34 mmol) in dichloromethane (15 mL). After this addition, 10 mL of aqueous sodium hydroxide (1 M) was added slowly and the reaction mixture was stirred for next 60 h at room temperature. After stirring was finished, another fraction of sodium hydroxide (10 mL, 1 M) was added rapidly. The reaction mixture was extracted with dichloromethane (3 × 25 mL) and combined organic portion was dried over anhydrous sodium sulfate. Evaporation of solvent led to isolation of the ligand L^1 as a dark orange oil. (1.13 g, Yield -79%) ^{1}H NMR (500 MHz, Methanol-d_4) 7.27 (m, 2H, pyridine ring), 7.50 (d, 2H, pyridine ring),7.76 (m, 2H, pyridine ring), 8.45 (d, 2H, pyridine ring), 3.68 (s, 4H,-N-CH_2-Py), 2.63 (s, 4H,-CH_2-CH_2-), 2.26 (s, 6H, N-CH_3).). IR (cm^{-1}): 2945, 2789, 1589, 1569, 1472, 1432, 1360, 1304, 1146, 1090, 1031, 994, 635, 614, 418.

L^2 **[N,N'-Dimethyl-N,N'-bis-(3,4-dimethoxy pyridine-2-ylmethyl)-1,2-diaminoethane].** The above mentioned protocol was adapted for preparation of ligand L^2. In a solution of 2-

(chloromethyl)-3,4-dimethoxypyridine hydrochloride (2.09 g, 9.34 mmol) in 10 mL of water, a solution of potassium bicarbonate(2.73 g, 19.74 mmol) in water (10 mL) was added dropwise. The reaction mixture was stirred at room temperature for next 30 minutes. After stirring is done, solution was extracted with dichloromethane (3 × 20 mL). The combined dichloromethane layer was treated with anhydrous sodium sulfate. The solution was filtered and solvent was removed by rotatory evaporation. The collected light yellow oil was dissolved in dichloromethane (10 ml). The 2-(chloromethyl)-3,4-dimethoxypyridine solution in dichloromethane was added dropwise to a solution of N, N′-Dimethylethylenediamine (0.503 mL, 4.67 mmol) in dichloromethane (15 mL). In the next step aqueous 1 M sodium hydroxide (10 mL) was slowly added and solution was stirred for additional 60 h at room temperature. After 60 h of stirring followed by the rapid addition of a second fraction of aqueous 1 M sodium hydroxide (10 mL, 10 mmol), the product was extracted with dichloromethane (3 × 25 mL).The combined organic layers were dried over anhydrous sodium sulfate and filtered. Subsequently, the excess solvent was evaporated by vacuum to afford yellow color viscous oil (Yield-1.86g, 89%). ^{1}H NMR (500 MHz, Methanol-*d_4*) 8.14 (d, 2H, pyridine ring), 7.05 (d, 2H, pyridine ring), 3.95 (s, 6H,-O-CH_3-Py), 3.85 (s, 6H,-O-CH_3-Py), 3.66 (s, 4H,-N-CH_2-Py), 2.67 (s, 4H, -CH_2-CH_2-), 2.26 (s, 6H, -N-CH_3). ^{13}C NMR (126 MHz, Methanol-*d*4) 160.77, 152.19, 147.28, 146.07 (d, J = 10.3 Hz), 108.87, 61.40, 58.17, 56.43, 56.07, 43.10. ESI-MS (in CH_3OH). observed *m/z* 391.3 [$(L^2+H)^+$] (*z* =1); theoretical-391.23 [$(L^2+H)^+$] (*z*=1). IR (cm^{-1}): 3375, 2945, 1626, 1584, 1447, 1425, 1261, 1228, 1173, 1073, 994, 828, 651, 603.

L^1Q [N,N’-Dimethyl-N,N’-bis-(quinoline-2-ylmethyl)-1,2-diaminoethane]. The ligand L^1Q was synthesized via similar procedure mentioned above.[23] To an aqueous solution of 2-(chloromethyl)-quinoline hydrochloride (2 g, 9.34 mmol), a solution of potassium carbonate

(2.73 g, 18.66 mmol) in 10 mL water was added in dropwise manner. The reaction mixture was stirred for 30 min at ambient temperature. After stirring, the resulting solution was extracted with dichloromethane (3 × 20 mL). The combined organic extracts were dried over anhydrous sodium sulfate and solvent was evaporates under vacuum. The product 2-(chloromethyl)-quinoline was then dissolved in dichloromethane (10 mL) and was added dropwise to a solution of N, N'-dimethylethylenediamine (0.503 mL, 5.34 mmol) in 15 mL dichloromethane. After this addition, aqueous sodium hydroxide (10 mL, 1 M) was added slowly. The reaction mixture was stirred for next 60 h at room temperature, followed by rapid addition of another fraction of sodium hydroxide (10 mL, 10 mmol). The reaction mixture was then extracted with dichloromethane (3 × 25 mL) and organic portions were combined and dried over anhydrous sodium sulfate. Volatile solvents were removed under vacuum to obtain crude ligand L^1Q as dark brown oil (1.68 g, Yield 85%). ^{1}H NMR (500 MHz, Methanol-d_4) 7.57 (m, 2H, quinoline ring),7.63 (d, 2H, quinoline ring), 7.73 (m, 2H, quinoline ring), 7.88 (d, 2H, quinoline ring),7.98 (d, 2H, quinoline ring), 8.21 (d, 2H, quinoline ring), 3.84 (s, 4H, -N-CH_2-Quinoline), 2.71 (s, 4H, -CH_2-CH_2-), 2.32 (s, 6H, -N-CH_3).). IR (cm^{-1}): 3384, 3056, 2946, 2800, 1617, 1598, 1564, 1504, 1456, 1426, 1361, 1309, 1223, 1141, 1119, 1032, 985, 951, 828, 784, 756, 619.

Synthesis of Ni(II) Complexes

[Ni(L^1)Cl_2] (1). The complex was prepared by following a published procedure.[21] A filtered solution of $NiCl_2$•$6H_2O$ (0.238 g, 1 mmol) in water (1 mL) was diluted with ethanol (2 mL) and heated for 15 min at 70 ºC. After 15 min., the solution was mixed with a solution of ligand L^1 (0.270 g, 1 mmol) in ethanol (1 mL). The resulting dark blue solution was kept inside the diethyl ether jar for ether vapor diffusion to produce blue green crystals (0.250 g, 0.625 mmol, Yield

63%). ESI-MS (in CH_3OH): Observed *m/z* 363.25 $[Ni(L^1) Cl]^+$ (*z* =1), theoretical 363.09. UV-Vis (in MeOH) $_{max}$ (• $M^{-1}cm^{-1}$:, 601 (15), 981 (28).

$[Ni(L^1Q)Cl_2]$ (2). To a solution of ligand L^1Q (0.400 g, 1.08 mmol) in methanol (4 mL), solution of $NiCl_2$•$6H_2O$ (0.257 g, 1.08 mmol) in methanol (5 mL) was added at room temperature. Within minutes of adding the $NiCl_2.6H_2O$ solution, light green precipitates began to form. After removal of solvent the green solid was isolated (0.270 g, 0.540 mmol, Yield 50 %). ESI-MS (in CH_3OH). Observed *m/z* 463.25 $[Ni(L^1Q) Cl]^+$ (*z* =1), Theoretical; 463.12. Anal. Calcd (%) for $C_{24}H_{26}Cl_2N_4Ni$: C 57.64, H 5.24, N 11.20, Cl 14.18. Found (%): C 57.42, H 5.19, N 11.16, Cl 13.95.UV-Vis UV-Vis (in MeOH) $_{max}$ (• $M^{-1}cm^{-1}$): 636 (18),1026 (11.4).

$[Ni(L^2)Cl_2]$ (3). The ligand L^2 (0.200 g, 0.512 mmol) dissolved in methanol (3 mL) was added dropwise to a stirring solution of $NiCl_2$•$6H_2O$ (0.122 g, 0.513 mmol) in methanol (5 mL). Dark green solution was obtained upon addition. Evaporation of solvent gave dark green color powder (0.157 g, 0.302 mmol, Yield-59%) ESI-MS (in CH_3OH). observed *m/z* 483.33 $[Ni(L^2) Cl]^+$ (*z* =1) theoretical 483.13 Anal. Calcd (%) for $C_{20}H_{34}Cl_3N_4NiO_5$. C 40.61, H 5.79, N 9.47, Cl 17.98 Found (%): C40.30, H 5.69, N 9.23, Cl 17.68.UV-Vis (in MeOH) $_{max}$ in nm(• $M^{-1}cm^{-1}$):611 (10), 969 (17).

Synthesis of Cu(II) Complexes

$[Cu(L^1)(ClO_4)_2]$ (4). Complex **4** was prepared by similar published procedure.[20] Addition of a solution of $Cu(ClO_4)_2$•$6H_2O$(0.371g, 1 mmol) in methanol (5 mL) to another a solution of ligand L^1 (0.270 g, 1 mmol) in 10 mL methanol followed by 10 minute stirring led to the formation of dark blue precipitates. The supernatant liquid was taken out and dark blue precipitates were dried under vacuum. Recrystallization from a mixture of hexane and acetonitrile by vapor diffusion afforded blue prism shaped crystals (0.308 g, 0.578 mmol, Yield-58%). ESI-MS (in CH_3CN). Observed *m/z* 432.12 $[Cu(L^1)\ ClO_4]^+$ (*z* =1) Theoretical- 432.06; observed 333.23$[Cu(L^1)]^+$ (*z* =1) theoretical 333.11. Anal. Calcd (%) for $C_{16}H_{22}Cl_2CuN_4O_8$: C 36.04, H 4.16, N 10.52, Cl 13.31. Found (%):C 36.31, H 4.25, N 10.48, Cl 13.12. UV-Vis (in MeCN) $_{max}$ in nm (• $M^{-1}cm^{-1}$): 624 (450).

$[Cu(L^1Q)(ClO_4)_2].3H_2O$ (5). The Cu $(ClO_4)_2$•$6H_2O$ (0.100 g, 0.270 mmol) dissolved in methanol (3 mL) was added to a stirring solution of ligand L^1Q (0.100 g, 0.270 mmol) in methanol (5 mL). The solvent was evaporated to isolate the solid. Solid crude material was washed with diethyl ether. Drying of solid under vacuum gave a dark green powder (0.133 g, 0.210 mmol, Yield - 78%) ESI-MS (in CH_3CN). Observed *m/z* 532.17 $[Cu(L^1Q)\ ClO_4]^+$ (*z* =1), Theoretical 532.09; Observed-433.33 $[Cu(L^1Q)]^+$ (*z* =1) Theoretical- 433.15. Anal. Calcd (%) for $C_{24}H_{32}Cl_2CuN_4O_{11}$: C 41.96, H 4.70, N 8.16, Cl 10.32. Found (%): C 42.03, H 4.36, N 8.02, Cl 11.23. UV-Vis (in MeCN) $_{max}$ in nm (• $M^{-1}cm^{-1}$): 626 (363).

$[Cu(L^2)(ClO_4)_2].3H_2O$ (6). A methanolic solution (3 mL) of $Cu(ClO_4)_2$•$6H_2O$ (0.190 g, 0.512 mmol) was added to a methanolic solution (5 mL) of ligand L^2 (0.200 g, 0.512 mmol). The final solution was stirred for 15 minutes at room temperature. Solvent evaporation led to appearance of blue solid particles. The isolated solid was dried under vacuum to give blue powder (0.271 g, 0.415 mmol, Yield- 80%). ESI-MS (in CH_3CN). Observed *m/z* 552.17 $[Cu(L^2)\ ClO_4]^+$ (*z* =1) Theoretical- 552.10. Anal. Calcd (%) for $C_{20}H_{36}Cl_2CuN_4O_{15}$: C 33.98, H 5.13, N 7.93, Cl 10.03. Found (%): C-34.09, H-5.05, N-7.93, Cl 9.91. UV-Vis (in MeCN) $_{max}$ in nm (•$M^{-1}cm^{-1}$):625 (301).

Supporting Information:

CCDC 1479598 and 1479597 contain the supplementary crystallographic data for complex **2** and **4**, respectively. These data can be obtained free of charge via Cambridge Crystallographic Data Center. Crystallographic data in CIF file format and detailed structural report on the crystals were available. The data of bond lengths calculated through computation studies are provided in detail in supporting information.

ABBREVIATIONS

EPR electron paramagnetic resonance, NMR nuclear magnetic resonance, BPMEN N,N-dimethyl-N.N'-bis-(pyridine-2-ylmethyl)1,2-diaminoethane, ESI-MS Electrospray ionization-mass spectrometry.

Author Information:

Corresponding author E-mail: anusree.mukherjee@uah.edu, vanheuvelen@g.hmc.edu.

The authors declare no competing financial interest.

Acknowledgement

This work was supported by grant supports from the University of Alabama in Huntsville. This material is based upon work supported by the U.S. Department of Energy, Office of Science, Office of Basic Energy Sciences, Division of Chemical Sciences, Geosciences, and Biosciences, through Grant DE-AC02-6CH11357 at Argonne National Laboratory. X-ray structural data was collected and analyzed by Dr. John Bacsa at Emory University - X-ray Crystallography Facility, Atwood Chemistry Center, 163 Emory University, Atlanta. This work used the Extreme Science and Engineering Discovery Environment (XSEDE), which is supported by National Science Foundation grant number ACI-1053575.

References

(1) Campbell, A. N.; Stahl, S. S. Overcoming the "Oxidant Problem": Strategies to Use O_2 as the Oxidant in Organometallic C-H Oxidation Reactions Catalyzed by Pd (and Cu). *Acc. Chem. Res.* **2012**, *45*, 851-863.

(2) Su, B.; Cao, Z.-C.; Shi, Z.-J. Exploration of Earth-Abundant Transition Metals (Fe, Co, and Ni) as Catalysts in Unreactive Chemical Bond Activations. *Acc. Chem. Res.* **2015**, *48*, 886-896.

(3) Stahl, S.; Labinger, J. A.; Bercaw, J. E. Homogeneous oxidation of alkanes by electrophilic late transition metals. *Angew. Chem., Int. Ed.* **1998**, *37*, 2181-2192.

(4) Rovasio, A.; Boggioni, L.; Tritto, I. Late-transition metal complexes with mixed NO, NS, NP chelating ligands for olefin polymerization catalysis. *Catal. Met. Complexes* **2011**, *35*, 27-118.

(5) Costas, M.; Tipton, A. K.; Chen, K.; Jo, D.-H.; Que, L., Jr. Modeling Rieske Dioxygenases: The First Example of Iron-Catalyzed Asymmetric cis-Dihydroxylation of Olefins. *J. Am. Chem. Soc.* **2001**, *123*, 6722-6723.

(6) Costas, M.; Mehn, M. P.; Jensen, M. P.; Que, L., Jr. Dioxygen Activation at Mononuclear Nonheme Iron Active Sites: Enzymes, Models, and Intermediates. *Chem. Rev. (Washington, DC, U. S.)* **2004**, *104*, 939-986.

(7) Liang, H.-C.; Dahan, M.; Karlin, K. D. Dioxygen-activating bio-inorganic model complexes. *Curr. Opin. Chem. Biol.* **1999**, *3*, 168-175.

(8) Hatcher, L. Q.; Karlin, K. D. Ligand influences in copper-dioxygen complex-formation and substrate oxidations. *Adv. Inorg. Chem.* **2006**, *58*, 131-184.

(9) Kleespies, S. T.; Oloo, W. N.; Mukherjee, A.; Que, L., Jr. C-H Bond Cleavage by Bioinspired Nonheme Oxoiron(IV) Complexes, Including Hydroxylation of n-Butane. *Inorg. Chem.* **2015**, *54*, 5053-5064.

(10) Chen, M. S.; White, M. C. A Predictably Selective Aliphatic C-H Oxidation Reaction for Complex Molecule Synthesis. *Science (Washington, DC, U. S.)* **2007**, *318*, 783-787.

(11) Chen, M. S.; White, M. C. Combined Effects on Selectivity in Fe-Catalyzed Methylene Oxidation. *Science (Washington, DC, U. S.)* **2010**, *327*, 566-571.

(12) Christmann, M. Selective oxidation of aliphatic C-H bonds in the synthesis of complex molecules. *Angew. Chem., Int. Ed.* **2008**, *47*, 2740-2742.

(13) Coates, C. M.; Hagan, K.; Mitchell, C. A.; Gorden, J. D.; Goldsmith, C. R. Structural characterization of manganese and iron complexes with methylated derivatives of bis(2-pyridylmethyl)-1,2-ethanediamine reveals unanticipated conformational flexibility. *Dalton Trans.* **2011**, *40*, 4048-4058.

(14) England, J.; Davies, C. R.; Banaru, M.; White, A. J. P.; Britovsek, G. J. P. Catalyst stability determines the catalytic activity of non-heme iron catalysts in the oxidation of alkanes. *Adv. Synth. Catal.* **2008**, *350*, 883-897.

(15) Costas, M.; Que, L., Jr. Ligand topology tuning of iron-catalyzed hydrocarbon oxidations. *Angew. Chem., Int. Ed.* **2002**, *41*, 2179-2181.

(16) Costas, M.; Rohde, J.-U.; Stubna, A.; Ho, R. Y. N.; Quaroni, L.; Muenck, E.; Que, L., Jr. A synthetic model for the putative FeIV2O2 diamond core of methane monooxygenase intermediate Q. *J. Am. Chem. Soc.* **2001**, *123*, 12931-12932.

(17) Company, A.; Gueell, M.; Popa, D.; Benet-Buchholz, J.; Parella, T.; Fontrodona, X.; Llobet, A.; Sola, M.; Ribas, X.; Luis, J. M.; Costas, M. Redox-Controlled Molecular Flipper Based on a Chiral Cu Complex. *Inorg. Chem.* **2006**, *45*, 9643-9645.

(18) Zhang, Y.; Xiang, L.; Wang, Q.; Duan, X.-F.; Zi, G. Synthesis, structure, and catalytic activity of chiral Cu(II) and Ag(I) complexes with (S,S)-1,2-diaminocyclohexane-based N4-donor ligands. *Inorg. Chim. Acta* **2008**, *361*, 1246-1254.

(19) Hureau, C.; Blondin, G.; Charlot, M.-F.; Philouze, C.; Nierlich, M.; Cesario, M.; Anxolabehere-Mallart, E. Synthesis, Structure, and Characterization of New Mononuclear Mn(II) Complexes. Electrochemical Conversion into New Oxo-Bridged Mn2(III,IV) Complexes. Role of Chloride Ions. *Inorg. Chem.* **2005**, *44*, 3669-3683.

(20) Pandiyan, T.; Guadalupe, H. J.; Cruz, J.; Bernes, S.; Ugalde-Salvdivar, V. M.; Gonzalez, I. DFT and experimental studies of perchlorate ion coordination in cis/trans-copper(II) complexes of tetradentate pyridyl ligands. *Eur. J. Inorg. Chem.* **2008**, 3274-3285.

(21) Kryatova, M. S.; Makhlynets, O. V.; Nazarenko, A. Y.; Rybak-Akimova, E. V. Nickel(II) complexes with tetradentate N4 ligands: Synthesis, structure, electrochemistry and thermochromism in solution. *Inorg. Chim. Acta* **2012**, *387*, 74-80.

(22) Abu-Surrah, A. S. Synthesis and characterization of some C2-symmetric copper(II), ruthenium(II) and chromium(0) complexes with quadridentate ligands having 2-quinolinyl auxiliary groups. *Asian J. Chem.* **2002**, *14*, 1251-1256.

(23) Iturrospe, A.; Artetxe, B.; Reinoso, S.; San Felices, L.; Vitoria, P.; Lezama, L.; Gutierrez-Zorrilla, J. M. Copper(II) Complexes of Tetradentate Pyridyl Ligands Supported on Keggin Polyoxometalates: Single-Crystal to Single-Crystal Transformations Promoted by Reversible Dehydration Processes. *Inorg. Chem.* **2013**, *52*, 3084-3093.

(24) Kalita, M.; Bhattacharjee, T.; Gogoi, P.; Barman, P.; Kalita, R. D.; Sarma, B.; Karmakar, S. Synthesis, Characterization, Crystal Structure and Bioactivities of a New Potential Tridentate (ONS) Schiff Base Ligand N-[2-(benzylthio)phenyl] salicylaldimine and its Ni(II), Cu(II) and Co(II) Complexes. *Polyhedron* **2013**, *60*, 47-53.

(25) Pattanayak, P.; Pratihar, J. L.; Patra, D.; Brandao, P.; Felix, V. Synthesis, crystal structure, spectral properties and catalytic activity of binuclear copper(II), mononuclear nickel(II) and cobalt(III) complexes containing Schiff base ligand. *Inorg. Chim. Acta* **2014**, *418*, 171-179.

(26) Bohle, D. S.; Zafar, A.; Goodson, P. A.; Jaeger, D. A. Synthesis and Characterization of Nickel(II) Bis(alkylthio)salen Complexes. *Inorg. Chem.* **2000**, *39*, 712-718.

(27) Lee, Y.; Lee, D.-H.; Narducci Sarjeant, A. A.; Zakharov, L. N.; Rheingold, A. L.; Karlin, K. D. Thioether Sulfur Oxygenation from O2 or H2O2 Reactivity of Copper Complexes with Tridentate N2Sthioether Ligands. *Inorg. Chem.* **2006**, *45*, 10098-10107.

(28) Addison, A. W.; Rao, T. N.; Reedijk, J.; Van Rijn, J.; Verschoor, G. C. Synthesis, structure, and spectroscopic properties of copper(II) compounds containing nitrogen-sulfur donor ligands: the crystal and molecular structure of aqua[1,7-bis(N-methylbenzimidazol-2'-yl)-2,6-dithiaheptane]copper(II) perchlorate. *J. Chem. Soc., Dalton Trans.* **1984**, 1349-1356.

(29) Zhao, Y.; Truhlar, D. G. The M06 suite of density functionals for main group thermochemistry, thermochemical kinetics, noncovalent interactions, excited states, and transition elements: two new functionals and systematic testing of four M06-class functionals and 12 other functionals. *Theor. Chem. Acc.* **2008**, *120*, 215-241.

(30) Krishnan, R.; Binkley, J. S.; Seeger, R.; Pople, J. A. Self-consistent molecular orbital methods. XX. A basis set for correlated wave functions. *J. Chem. Phys.* **1980**, *72*, 650-654.

(31) Ditchfield, R.; Hehre, W. J.; Pople, J. A. Self-consistent molecular-orbital methods. IX. Extended Gaussian-type basis for molecular-orbital studies of organic molecules. *J. Chem. Phys.* **1971**, *54*, 724-728.

(32) Knight, P. D.; Scott, P. Predetermination of chirality at octahedral centres with tetradentate ligands: prospects for enantioselective catalysis. *Coord. Chem. Rev.* **2003**, *242*, 125-143.

(33) Harvey, J. N. On the accuracy of density functional theory in transition metal chemistry. *Annu. Rep. Prog. Chem., Sect. C: Phys. Chem.* **2006**, *102*, 203-226.

(34) Guadalupe Hernandez, H. J.; Pandiyan, T.; Bernes, S. Mercaptoethanesulfonic acid (CoM imitator) interaction studies with nickel(II) complexes of pyridyl groups containing tetradentate ligands: Synthesis, structure, spectra and redox properties. *Inorg. Chim. Acta* **2006**, *359*, 1-12.

(35) Anacona, J. R.; Marquez, V. E.; Jimenez, Y. Synthesis and characterization of manganese(II), nickel(II), copper(II) and zinc(II) Schiff-base complexes derived from 1,10-phenanthroline-2,9-dicarboxaldehyde and 2-mercaptoethylamine. *J. Coord. Chem.* **2009**, *62*, 1172-1179.

(36) Mautner, F. A.; Mikuriya, M.; Ishida, H.; Sakiyama, H.; Louka, F. R.; Humphrey, J. W.; Massoud, S. S. Dicyanamido-metal(II) complexes. Part 4: Synthesis, structure and magnetic characterization of polynuclear Cu(II) and Ni(II) complexes bridged by μ-1,5-dicyanamide. *Inorg. Chim. Acta* **2009**, *362*, 4073-4080.

(37) Liu, W.; Migdisov, A.; Williams-Jones, A. The stability of aqueous nickel(II) chloride complexes in hydrothermal solutions: Results of UV-Visible spectroscopic experiments. *Geochim. Cosmochim. Acta* **2012**, *94*, 276-290.

(38) Gurumoorthy, P.; Mahendiran, D.; Kalilur Rahiman, A. Theoretical calculations, DNA interaction, topoisomerase I and phosphatidylinositol-3-kinase studies of water soluble mixed-ligand nickel(II) complexes. *Chem.-Biol. Interact.* **2016**, *248*, 21-35.

(39) Sadhu, M. H.; Solanki, A.; Kumar, S. B. Mixed ligand complexes of copper(II), cobalt(II), nickel(II) and zinc(II) with thiocyanate and pyrazole based tetradentate ligand: Syntheses, characterizations and structures. *Polyhedron* **2015**, *100*, 206-214.

(40) Mahendrasinh, Z.; Ankita, S.; Kumar, S. B.; Escuer, A.; Suresh, E. Cyanato bridged binuclear nickel(II) and copper(II) complexes with pyridylpyrazole ligand: Synthesis, structure and magnetic properties. *Inorg. Chim. Acta* **2011**, *375*, 333-337.

(41) Brudenell, S. J.; Spiccia, L.; Tiekink, E. R. T. Binuclear Copper(II) Complexes of Bis(pentadentate) Ligands Derived from Alkyl-Bridged Bis(1,4,7-triazacyclononane) Macrocycles. *Inorg. Chem.* **1996**, *35*, 1974-1979.

(42) McLachlan, G. A.; Fallon, G. D.; Martin, R. L.; Spiccia, L. Synthesis, Structure and Properties of Five-Coordinate Copper(II) Complexes of Pentadentate Ligands with Pyridyl Pendant Arms. *Inorg. Chem.* **1995**, *34*, 254-261.

(43) Massoud, S. S.; Louka, F. R.; David, R. N.; Dartez, M. J.; Nguyn, Q. L.; Labry, N. J.; Fischer, R. C.; Mautner, F. A. Five-coordinate metal(II) complexes based pyrazolyl ligands. *Polyhedron* **2015**, *90*, 258-265.

(44) Massoud, S. S.; Louka, F. R.; Nguyen, L.-T.; Mikuriya, M.; Albering, J. H.; Mautner, F. A. Structural and magnetic characterization of 1-D complexes constructed from pyrazole-3,5-dicarboxylate bridging multi copper(II) centers. *Inorg. Chim. Acta* **2011**, *366*, 394-398.

(45) Jacobson, R. R.; Tyeklar, Z.; Karlin, K. D.; Zubieta, J. Fluoride as a terminal and bridging ligand for copper: isolation and x-ray crystallographic characterization of copper monomeric and dimeric complexes [CuII(TMPA)F]nn+ (n = 1 or 2; TMPA = tris[(2-pyridyl)methyl]amine). *Inorg. Chem.* **1991**, *30*, 2035-2040.

(46) Mukhopadhyay, U.; Bernal, I.; Massoud, S. S.; Mautner, F. A. Syntheses, structures and some electrochemistry of Cu(II) complexes with tris[(2-pyridyl)methyl]amine: [Cu{N(CH2-py)3}(N3)]ClO4 (I), [Cu{N(CH2-py)3}(O-NO)]ClO4 (II) and [Cu{N(CH2-py)3}(NCS)]ClO4 (III). *Inorg. Chim. Acta* **2004**, *357*, 3673-3682.

(47) Hathaway, B. J. Correlation of the electronic properties and stereochemistry of mononuclear [CuN4-6] chromophores. *J. Chem. Soc., Dalton Trans.* **1972**, 1196-1199.

(48) Kaur, A.; Ribelli, T. G.; Schroder, K.; Matyjaszewski, K.; Pintauer, T. Properties and ATRP Activity of Copper Complexes with Substituted Tris(2-pyridylmethyl)amine-Based Ligands. *Inorg. Chem.* **2015**, *54*, 1474-1486.

(49) Ohtsu, H.; Tanaka, K. Equilibrium of Low- and High-Spin States of Ni(II) Complexes Controlled by the Donor Ability of the Bidentate Ligands. *Inorg. Chem.* **2004**, *43*, 3024-3030.

(50) Chandra, S.; Gupta, L. K. EPR and electronic spectral studies on Co(II), Ni(II) and Cu(II) complexes with a new tetradentate [N4] macrocyclic ligand and their biological activity. *Spectrochim. Acta, Part A* **2004**, *60A*, 1563-1571.

(51) Patel, R. N.; Shukla, K. K.; Singh, A.; Choudhary, M.; Chauhan, U. K.; Dwivedi, S. Copper(II) complexes as superoxide dismutase mimics: Synthesis, characterization, crystal structure and bioactivity of copper(II) complexes. *Inorg. Chim. Acta* **2009**, *362*, 4891-4898.

(52) Husarikova, L.; Repicka, Z.; Moncol, J.; Valigura, D.; Valko, M.; Mazur, M. Unusual EPR Spectra with Inverse Axial g values of Chlorosalicylate-Cu(II)-2,6-Pyridinedimethanol Complex in Frozen Water-Methanol Solution. *Appl. Magn. Reson.* **2013**, *44*, 571-582.

(53) Bertini, I.; Gatteschi, D.; Scozzafava, A. Six-coordinate copper complexes with g•<g⊥ in the solid state. *Coord. Chem. Rev.* **1979**, *29*, 67-84.

(54) Hathaway, B. J.; Billing, D. E. Electronic properties and stereochemistry of mononuclear complexes of the copper(II) ion. *Coord. Chem. Rev.* **1970**, *5*, 143-207.

(55) Garribba, E.; Micera, G. The determination of the geometry of Cu(II) complexes. An EPR spectroscopy experiment. *J. Chem. Educ.* **2006**, *83*, 1229-1232.

(56) Pilbrow, J. R.: *Transition Ion Electron Paramagnetic Resonance* Oxford University Press.

(57) Salavati-Niasari, M.; Mirsattari, S. N. Synthesis, characterization and catalytic oxyfunctionalization of cyclohexene with tert-butylhydroperoxide and hydrogen peroxide in the presence of alumina-supported Mn(II), Co(II), Ni(II) and Cu(II) bis(2-hydroxyanil)benzil complexes. *J. Mol. Catal. A: Chem.* **2007**, *268*, 50-58.

(58) Salavati-Niasari, M.; Banitaba, S. H. Alumina-supported Mn(II), Co(II), Ni(II) and Cu(II) bis(2-hydroxyanil)acetylacetone complexes as catalysts for the oxidation of cyclohexene with tert-butyl hydroperoxide. *J. Mol. Catal. A: Chem.* **2003**, *201*, 43-54.

(59) Yokoyama, T.; Yoshise, M.; Hase, S.; Kawate, A.; Akashi, H.; Zenki, M. Crystal structure of isothiocyanato-N,N'-dimethyl-N,N'-bis(pyridine-2-ylmethyl)propane-1,3-diaminecopper(II) perchlorate. *X-Ray Struct. Anal. Online* **2011**, *27*, 51-52.

(60) Yokoyama, T.; Hase, S.; Yoshise, M.; Shiomi, A.; Shiba, T.; Akashi, H.; Zenki, M. Crystal structure of isothiocyanato-N,N'-diethyl-N,N'-bis(pyridine-2-ylmethyl)propanediaminecopper(II) perchlorate. *X-Ray Struct. Anal. Online* **2011**, *27*, 65-66.

(61) Yokoyama, T.; Yoshise, M.; Hase, S.; Akashi, H.; Zenki, M. Crystal structure of catena-(μ2-perchlorato)-N-ethyl-N,N'-bis(pyridin-2-ylmethyl)propane-1,3-diaminecopper(II) perchlorate. *X-Ray Struct. Anal. Online* **2012**, *28*, 47-48.

(62) Stoll, S.; Schweiger, A. EasySpin, a comprehensive software package for spectral simulation and analysis in EPR. *J. Magn. Reson.* **2006**, *178*, 42-55.

(63) Bain, G. A.; Berry, J. F. Diamagnetic corrections and Pascal's constants. *J. Chem. Educ.* **2008**, *85*, 532-536.

(64) Sheldrick, G. M. SHELXT - Integrated space-group and crystal-structure determination. *Acta Crystallogr., Sect. A: Found. Adv.* **2015**, *71*, 3-8.

(65) Dolomanov, O. V.; Bourhis, L. J.; Gildea, R. J.; Howard, J. A. K.; Puschmann, H. OLEX2: a complete structure solution, refinement and analysis program. *J. Appl. Crystallogr.* **2009**, *42*, 339-341.

(66) Sheldrick, G. M. A short history of SHELX. *Acta Crystallogr., Sect. A: Found. Crystallogr.* **2008**, *64*, 112-122.

(67) Frisch, M. J.; Trucks, G. W.; Schlegel, H. B.; Scuseria, G. E.; Robb, M. A.; Cheeseman, J. R.; Scalmani, G.; Barone, V.; Mennucci, B.; Petersson, G. A.; Nakatsuji, H.; Caricato, M.; Li, X.; Hratchian, H. P.; Izmaylov, A. F.; Bloino, J.; Zheng, G.; Sonnenberg, J. L.; Hada, M.; Ehara, M.; Toyota, K.; Fukuda, R.; Hasegawa, J.; Ishida, M.; Nakajima, N.; Honda, Y.; Kitao, O.; Nakai, H.; Vreven, T.; Montgomery, A.; Peralta, J. E.; Ogliaro, F.; Bearpark, M.; Heyd, J. J.; Brothers, E.; Kudin, K. N.; Staroverov, V. N.; Keith, T.; Kobayashi, R.; Normand, J.; Raghavachari, K.; Rendell, A.; Burant, J. C.; Iyengar, S. S.; Tomasi, J.; Cossi, M.; Rega, N.; Millam, J. M.; Klene, M.; Knox, J. E.; Cross, J. B.; Bakken, V.; Adamo, C.; Jaramillo, J.; Gomperts, R.; Stratmann, R. E.; Yazyev, O.; Austin, A. J.; Cammi, R.; Pomelli, C.; Ochterski, J. W.; Martin, R. L.; Morokuma, K.; Zakrzewski, V. G.; Voth, G. A.; Salvador, P.; Dannenberg, J. J.; Dapprich, S.; Daniels, A. D.; Farkas, O.; Foresman, J. B.; Ortiz, J. V.; Cioslowski, J.; Fox, D. J.: Gaussian 09, Revision D.01. Gaussian, I., Ed.: Wallingford, CT, 2013.

(68) Towns, J.; Cockerill, T.; Dahan, M.; Foster, I.; Gaither, K.; Grimshaw, A.; Hazlewood, V.; Lathrop, S.; Lifka, D.; Peterson, G. D.; Roskies, R.; Scott, J. R.; Wilkins-Diehr, N. XSEDE: Accelerating Scientific Discovery. *Computing in Science & Engineering* **2014**, *16*, 62-74.

Graphical Abstract:

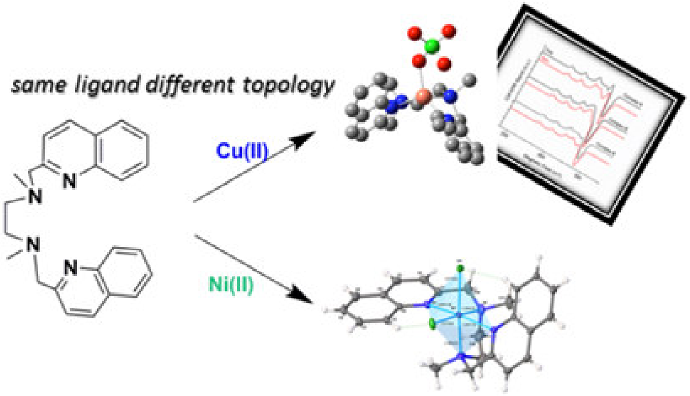

Graphical Abstract (For review purposes)

Ni(II) and Cu(II) coordination complexes supported by tetradentate ligands with pyridine functionality are underrepresented in the literature. This article defines the synthesis and characterization of late transition metal complexes supported by ligands from bispicen family. This paper also reports the first X-ray crystal structure of a new nickel complex supported by a sterically demanding tetradentate ligand and its detailed theoretical and spectroscopic characterization.

Highlights:

- A series of mononuclear nickel (II) and copper (II) complexes containing N,N’-dimethyl-N,N’-bis-(pyridine-2-ylmethyl)-1,2-diaminoethane ligand and its derivatives have been prepared.
- Structural data along with theoretical calculation on these coordination complexes revealed different geometries based on the central metal ion.
- Synthesis of a new bispicen ligand derivative with more electron-donating groups in the pyridine ring is reported.